# Arbuscular mycorrhizal fungi community analysis revealed the significant impact of arsenic in antimony- and arsenic-contaminated soil in three Guizhou regions

Yidong Mi[1,2], Chao Xu[3], Xinru Li[1,4], Min Zhou[1,2], Ke Cao[1], Cuimin Dong[1], Xuemei Li[1], Ningning Ji[1], Fanfan Wang[1], Hailei Su[1], Xuesong Liu[1] and Yuan Wei[1]*

[1]State Key Laboratory of Environmental Criteria and Risk Assessment, Chinese Research Academy of Environmental Sciences, Beijing, China, [2]College of Environment, Hohai University, Nanjing, China, [3]Chinese Research Academy of Environmental Sciences, Beijing, China, [4]College of Environmental Science and Engineering, Tongji University, Shanghai, China

**Introduction:** The lack of systematic investigations of arbuscular mycorrhizal fungi (AMF) community composition is an obstacle to AMF biotechnological applications in antimony (Sb)- and arsenic (As)-polluted soil.

**Methods:** Morphological and molecular identification were applied to study the AMF community composition in Sb- and As-contaminated areas, and the main influencing factors of AMF community composition in Sb- and As-contaminated areas were explored.

**Results:** (1) A total of 513,546 sequences were obtained, and the majority belonged to Glomeraceae [88.27%, 193 operational taxonomic units (OTUs)], followed by Diversisporaceae, Paraglomeraceae, Acaulosporaceae, Gigasporaceae, and Archaeosporaceae; (2) the affinity between AMF and plants was mainly related to plant species ($F = 3.488$, $p = 0.022 < 0.050$), which was not significantly correlated with the total Sb (TSb) and total As (TAs) in soil; (3) the AMF spore density was mainly related to the available nitrogen, available potassium, and total organic carbon; (4) The effect of soil nutrients on AMF community composition (total explanation: 15.36%) was greater than that of soil Sb and As content (total explanation: 5.80%); (5) the effect of TAs on AMF community composition ($\lambda = -0.96$) was more drastic than that of TSb ($\lambda = -0.21$), and the effect of As on AMF community composition was exacerbated by the interaction between As and phosphorus in the soil; and (6) Diversisporaceae was positively correlated with the TSb and TAs.

**Discussion:** The potential impact of As on the effective application of mycorrhizal technology should be further considered when applied to the ecological restoration of Sb- and As-contaminated areas.

KEYWORDS

arbuscular mycorrhizal fungi, antimony, arsenic, bioremediation, community composition

# 1. Introduction

Antimony (Sb) and arsenic (As) have similar chemical characteristics (Anawar et al., 2011; Yu et al., 2021) and occur ubiquitously in the environment at trace levels (Johnston et al., 2020; Xu et al., 2020; Li Y. et al., 2021). Both Sb and As have been listed as priority pollutants by the European Union and the Environmental Protection Agency of the USA and restricted pollutants by China (Wei et al., 2015a; Chang et al., 2022; Yang et al., 2022; Zhou et al., 2022). Sb is carcinogenic and excessive Sb exposure can damage the respiratory, cardiovascular, and urinary systems (Nishad and Bhaskarapillai, 2021; Liu et al., 2022; Zhou et al., 2022). China is the world's largest producer of Sb, especially southwest China, which accounts for 80% of global Sb production (Xu et al., 2020). Sb is typically accompanied by As in sulfide ores in Sb mining areas, which are found worldwide (Li et al., 2017; Chang et al., 2022). As is also a metalloid and a primary environmental pollutant and carcinogen (Li B. et al., 2021; Ozturk et al., 2022; Wu et al., 2022). The Qinglong Sb mine is a typical Sb mining area in southwest China, where the concentrations of soil Sb and As reach as high as 5,447 and 472 mg/kg, respectively, which are much higher than the Chinese background soil value of Chinese values (Mao et al., 2022), which has affected the residents living near the Qinglong Sb mine. The consumption of contaminated foods or drinking water was found to be the dominant dietary intake source of Sb and As for the residents near an Sb mining area, for whom the total dietary intakes were 554 and 306 μg/day, respectively (Wu et al., 2011; Chang et al., 2022). Reducing Sb and As exposure and the subsequent harm to the human body urgently need to be addressed.

There are a variety of microorganisms in the ecosystem that can mutualism with plants and play a role in the resistance of plants to biotic and abiotic stresses (Xiao et al., 2022; Yan et al., 2022). Arbuscular mycorrhizal fungi (AMF) are ubiquitous in soil environments and interact with most plants through mycorrhizal structures (Xiao et al., 2022). The application of AMF to enhance plant resistance to heavy metal toxicity and improve phytoremediation efficiency is an ecologically friendly soil remediation technology that has been widely researched (Gu et al., 2017; Bi et al., 2019; Riaz et al., 2021). Currently, there are two common strategies for the application of AMF to reduce human exposure to Sb or As. The first strategy is to use AMF to enhance the Sb and As enrichment of plants (Wei et al., 2016; Liu et al., 2020) or to improve the Sb or As tolerance of plants (Zhang and Chen, 2021; Xi et al., 2022), so as to reduce the content or toxicity of Sb or As in soil, and finally realize the ecological restoration of Sb- or As-polluted areas. Another strategy is to use AMF to reduce Sb or As migration into agricultural products or to convert Sb or As into less toxic forms to reduce human exposure to Sb or As (Alam et al., 2019; Li et al., 2022). Therefore, the rational application of AMF has great significance for ecological restoration and food security around Sb- and As-contaminated areas.

Considering the key role of AMF in soil ecosystems, it is important to understand the community composition and diversity distribution of AMF in Sb- and As-contaminated areas and the effects of Sb and As on AMF for ecological restoration and food security around Sb- and As-contaminated areas. Wei et al. (2015a) investigated the AMF of a typical Sb mining area in China

and concluded that Sb contamination was the dominating factor influencing the AMF community composition in the Sb mining area. However, this study ignored the potential effect of As in the Sb mining area. Schneider et al. (2013) studied AMF communities in an As-contaminated area of Brazil, and they found that As contamination reduced the AMF species richness, but the effects of other soil factors on the AMF community composition were not systematically discussed. Parvin et al. (2019) conducted a detailed analysis of the effects of As pollution on the AMF community composition in paddy fields in Bangladesh. However, the results of this study have little significance for the application of AMF in the ecological restoration of Sb and As mining areas. The lack of research on AMF community composition and its influencing factors in Sb- and As-co-contaminated areas is an obstacle to the effective implementation of ecological remediation technology in Sb- and As-contaminated areas.

The Qinglong Sb mine in Guizhou Province is one of the main Sb mining areas in China, and it has been exploited for nearly 60 years. Historical mining and smelting activities in the Qinglong Sb mine have caused serious Sb and As pollution that threatens the health of nearby residents (Liu et al., 2011). The preliminary survey found that AMF was widely distributed in this area, thus making the study area an ideal system for the evaluation of AMF community composition in Sb- and As-contaminated soil systems. In this study, the AMF community composition was characterized using high-throughput sequencing technology in three sites with different Sb and As concentrations. The study aimed to (1) identify the factors affecting the AMF-plant symbiosis in Sb- and As-contaminated areas and explore the effects of Sb and As pollution on the AMF colonization rate and spore density; (2) investigate the relationship between the soil properties and the AMF community composition and identify the main factors affecting the AMF community composition in Sb- and As-contaminated areas; and (3) screen the dominant AMF in Sb- and As-contaminated areas for ecological restoration in Sb- and As-contaminated areas.

# 2. Materials and methods

## 2.1. Study area and soil sampling

Samples were collected in the Qinglong Sb mining area, which is situated in Qinglong County, Qianxinan Buyei and Miao Autonomous Prefecture, Guizhou Province, China. This area belongs to a karst landform with abundant groundwater, and has a plateau subtropical climate, with a mean annual temperature of 14.1°C and mean annual rainfall of 1,500 mm.

Samples were collected in August 2021. Based on the preliminary investigation, three sampling sites were selected according to the mining function, namely S1, S2, and S0. S1 was the smelting area with a total Sb (TSb) of 3,800–27,300 mg/kg and total As (TAs) of 193–1,160 mg/kg. S2 was the tailings pond with a TSb of 2,640–48,000 mg/kg and TAs of 1,090–2,980 mg/kg. The undisturbed site S0 was located over 1 km away from the mining area. The sampling point information is shown in **Figure 1** and **Supplementary Table 1**. The TSb of S0 (405.89 mg/kg) was slightly higher than the second type of land control value limit specified in the risk control standard for soil contamination of

development land of China (360 mg/kg) (Ministry of Ecology and Environment of the People's Republic of China, 2018), and the TAs of S0 (85.03 mg/kg) was lower than the first type of land control value limit specified in the risk control standard for the soil contamination of development land of China (120 mg/kg) (Ministry of Ecology and Environment of the People's Republic of China, 2018). Four 20 m × 20 m plots were selected at S1 and S2, and three plots were selected at S0. Dominant plant and 1 kg rhizosphere soil samples were collected from the topsoil (0–10 cm) associated with *Artemisia argyi* (Aa), *Rumex acetosa* (Ra), *Boehmeria nivea* (Bn), *Buddleja lindleyana* (Bl), and *Carpesium abrotanoides* (Ca). Three well-grown individuals of each plant species were collected from each plot and mixed into one sample. The dominant plants selected at each sampling site are shown in **Supplementary Table 1**. Each sample was then divided into two subsamples, with one refrigerated in liquid nitrogen and sent immediately to the laboratory for molecular analysis and the other was used to analyze the spore density and soil properties after air-drying. The roots of plants were used to measure the AMF colonization rate.

## 2.2. Measurement of soil properties, AMF colonization rate, and spore density

The alkali N-proliferation method was used to measure available nitrogen (AN). Briefly, 2 g of air-dried soil was alkalized with 10 ml 1.8 mol/L NaOH solution and the alkalized products were absorbed with 3 ml 20 g/L $H_3BO_3$ indicator and titrated with 0.01 mol/L HCl solution. Extraction with $NH_4F$-HCl solution (pH < 6.5) or $NaHCO_3$ solution (pH > 6.5) and estimation using the molybdenum-antimony colorimetric method was utilized to determine available phosphorus (AP). The total calcium (TCa) was measured with an inductively coupled plasma optical emission spectrometer (ICP-OES, 5110, Agilent Technologies, Santa Clara, CA, USA), and the available potassium (AK) was estimated with the ammonium acetate method and flame photometry (AA-6880, Shimadzu, Shanghai, China). The soil total organic carbon (TOC) was measured using a TOC analyzer (Vario TOC Select, Elementar, Beijing, China). The soil pH and electrical conductivity (EC) were estimated with a pH meter (FE28, Mettler Toledo, Shanghai, China) after adding 25 ml of water to 10 g of air-dried soil.

The TSb and TAs were extracted by adding 6 ml of aqua regia (1.5 ml HCl and 4.5 ml $HNO_3$) to 0.1 g dry soil sample and were digested using a microwave digestion system (Mars 6 Classic 910980, CEM, Charlotte, NC, USA). The digestion procedure consisted of heating for 5 min and maintaining a temperature of 120°C for 2 min; heating for 4 min and maintaining 150°C for 5 min; and heating for 5 min and maintaining 185°C for 40 min. The extract was filtered through a 0.45-μm nylon filter, diluted to 50 ml with pure water, and analyzed using inductively coupled plasma mass spectrometry (ICP-MS, 7900, Agilent Technologies, Santa Clara, CA, USA). The diethylenetriamine pentaacetic acid (DTPA)-extractable Sb (DTPA-Sb) and DTPA-extractable As (DTPA-As) concentrations were determined by ICP-OES (5110, Agilent Technologies, Santa Clara, CA, USA) after a 10 g sample was dissolved using DTPA extraction agent [DTPA (0.005 M), $CaCl_2$ (0.01 M), and triethanolamine

(TEA, 0.1 M, pH 7.3)]. All of the soil data are shown in **Table 1**.

The AMF colonization rates were measured according to Vierheilig et al. (2005). In brief, roots were cleaned and cut into 2-cm segments. Then the root segments were transferred to 10% potassium hydroxide (KOH) and heated in a 90°C water bath for 1 h. The root segments were stained with 5% ink-vinegar for 5 min, cleaned with tap water that contained several drops of acetic acid, and observed under a microscope (NSZ-810, Beijing East-Bio Technology Co. Ltd., Beijing, China). Spores were isolated from approximately 20 g of a soil sample via wet sieving, decanting, and centrifugation (3,000 rpm, 2 min) through a 60% (weight/volume) sucrose cushion. Spores were counted using a microscope (NSZ-810, Beijing East-Bio Technology Co. Ltd., Beijing, China).

## 2.3. DNA extraction, polymerase chain reaction (PCR) amplification, and sequencing

Total DNA was extracted from 0.25 g soil with an E.Z.N.A.® soil DNA Kit (Omega Bio-Tek, Beijing, China) according to the manufacturer's instructions. The 18S rRNA of AMF was subjected to two-step nested PCR. The PCR program and reaction system components are shown in **Supplementary Table 2**. AML1: 5′-ATCAACTTTCGATGGTAGGATAGA-3′ and AML2: 5′-GAACCCAAACACTTTGGTTTCC-3′ were used as primers in the first-round PCR, and AMV4.5NF: 5′-AAGCTCGTAGTTGAATTTCG-3′ and AMDGR: 5′-CCCAACTATCCCTATTAATCAT-3′ were used as primers in the second-round PCR. The PCR products were purified using an AxyPrep DNA Gel Extraction Kit (Axygen Biosciences, Union City, CA, USA) and quantified using QuantiFluor-ST (Promega, Beijing, China). Purified amplicons were sequenced using an Illumina MiSeq platform (Majorbio, Shanghai, China) via 2 × 250 bp paired-end sequencing. Raw reads have been submitted to the NCBI sequence read archive (SRA) database with the following accession number: PRJNA943530.

Sequences were demultiplexed as fastq files and quality-filtered using a QIIME pipeline (version 1.17) (Xiao B. et al., 2019). Sequences were clustered into operational taxonomic units (OTUs) at 97% sequence similarity, and the chimeric sequences were removed using the UPARSE program (version 7.1).[1] The taxonomic classification of each 18S rRNA gene sequence was analyzed with the Ribosomal Database Project classifier[2] against the MaarjAM 18S rRNA database (Amato et al., 2013).

## 2.4. Statistical and data analysis

Data analyses were performed with the SPSS 17.0 software package. Differences between the means of soil properties were assessed using analysis of variance (ANOVA) tests, and the Duncan test was used to compare the homogeneity of variance at the

---

[1] http://drive5.com/uparse/
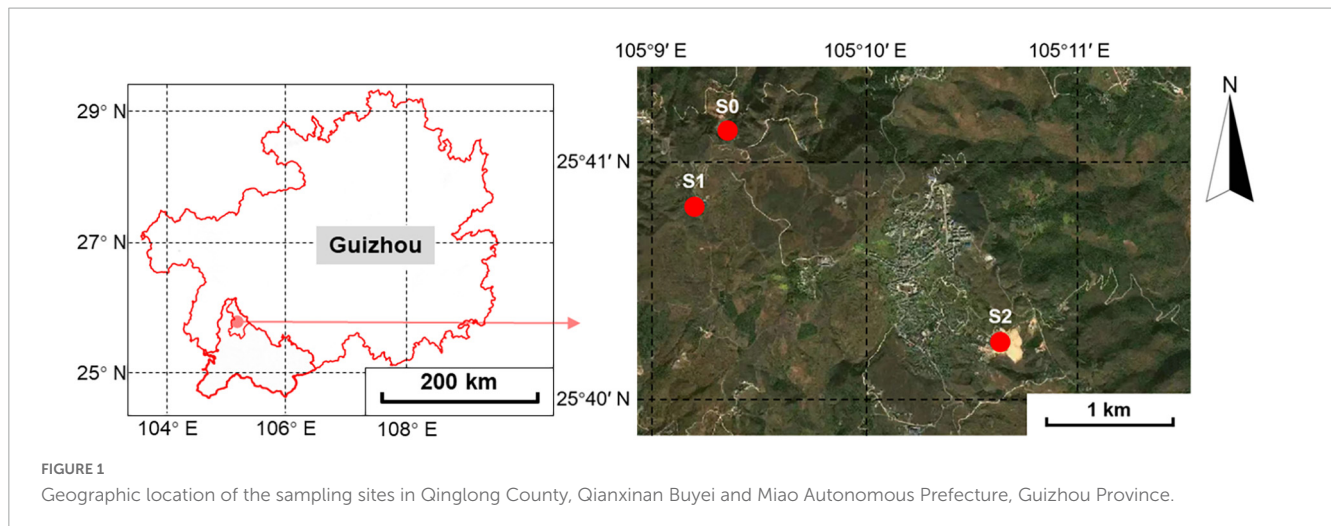
[2] http://rdp.cme.msu.edu/

FIGURE 1
Geographic location of the sampling sites in Qinglong County, Qianxinan Buyei and Miao Autonomous Prefecture, Guizhou Province.

TABLE 1 Physicochemical properties of the sampling sites.

| Sampling site | AN (mg/kg) | AP (mg/kg) | AK (mg/kg) | TOC (g/kg) |
|---|---|---|---|---|
| S0 | $155.56 \pm 28.44^b$ | $1.35 \pm 0.25^b$ | $250.22 \pm 58.64^b$ | $30.867 \pm 6.981^b$ |
| S1 | $343.17 \pm 103.35^a$ | $8.50 \pm 12.04^b$ | $398.17 \pm 133.48^a$ | $74.438 \pm 54.580^a$ |
| S2 | $39.73 \pm 22.23^c$ | $64.00 \pm 25.23^a$ | $182.33 \pm 47.15^b$ | $16.138 \pm 22.759^b$ |
| Sampling site | TSb (g/kg) | DTPA-Sb (mg/kg) | TAs (g/kg) | DTPA-As (mg/kg) |
| S0 | $0.406 \pm 0.153^b$ | $0.25 \pm 0.23^b$ | $0.085 \pm 0.014^c$ | $0.26 \pm 0.18$ |
| S1 | $12.311 \pm 7.255^a$ | $10.85 \pm 14.56^{ab}$ | $0.614 \pm 0.347^b$ | $0.35 \pm 0.28$ |
| S2 | $20.053 \pm 14.370^a$ | $16.83 \pm 14.58^a$ | $2.103 \pm 0.681^a$ | $0.30 \pm 0.24$ |
| Sampling site | pH | EC (mS/m) | TCa (g/kg) | – |
| S0 | $7.18 \pm 0.37$ | $5.14 \pm 3.50^b$ | $8.797 \pm 2.639^c$ | – |
| S1 | $7.36 \pm 0.61$ | $9.46 \pm 3.05^b$ | $33.858 \pm 26.351^b$ | – |
| S2 | $7.29 \pm 0.50$ | $128.69 \pm 46.25^a$ | $59.242 \pm 18.478^a$ | – |

Different lowercase letters indicate significant differences at $p < 0.05$.

0.05 probability level ($p = 0.05$). The observed richness (Sobs), Shannon, Shannoneven, and Coverage indexes were calculated using Mothur (Version 1.80.2).[3] The AMF colonization rate, spore density, and the Sobs, Shannon, Shannoneven, and Coverage index box plots were constructed using R, and the significance of the differences were tested using an ANOVA test. The significance levels (F values) of the effects of plants, sampling sites, and their interactions on the AMF colonization rate, spore density, and AMF community index were tested using multi-way ANOVA analysis. The AMF community bar plot at the family level was plotted with R. Principal coordinates analysis (PCoA) was employed to illustrate AMF community composition clustering using the R package based on the Bray–Curtis distance. Permutational multivariate ANOVA (PERMANOVA) and analysis of similarities (ANOSIM) based on the Bray–Curtis distance were conducted to analyze the significant difference in the AMF community compositions among the sampling sites. The rarefaction curve was performed using R. Heat trees were generated using the log2 ratios of the median counts for each taxon and the Wilcox rank-sum test followed by

a Benjamini and Hochberg correction for multiple testing using the "Metacoder" package in R (Foster et al., 2016). The variance inflation factor (VIF) was calculated in SPSS 17.0 and used to diagnose multicollinearity, environmental factors with VIF > 10 were screened for canonical correlation analysis (CCA) analysis (Guzman et al., 2021). The correlation between soil properties and AMF communities was elucidated through CCA using the R package. Variation partitioning analysis (VPA) was conducted in R using the "vegan" package to partition the influences of soil nutrients, heavy metals, and pH and TCa on AMF community composition. A Mantel test was used to compare the correlations between soil properties and the AMF colonization rate, spore density, and the Sobs, Shannon, and Shannoneven indexes, and between soil properties and AMF families in R using the "ggcor" package. The correlations between the soil properties and the AMF colonization rate, spore density, and the Sobs, Shannon, and Shannoneven indexes were obtained based on the Pearson correlation coefficient. Two-factor correlation network analysis was performed using Gephi 0.9.7. The heatmaps were created using the R package and the correlations were obtained based on the Pearson correlation coefficient. To estimate the direct and indirect effects of the soil properties on the AMF richness and

---

3 https://mothur.org/wiki/calculators/

diversity and spore density, a structural equation model (SEM) was fitted to the data using AMOS (IBM SPSS AMOS 26). The soil nutrients were synthetic variables derived from the first principal components generated by the principal component analysis (PCA) of AN, AK, and TOC (total explainable variance = 81.5%); the AMF richness and diversity were synthetic variables derived from the first principal components generated through PCA of the Sobs, Shannon, and the Shannoneven indexes (total explainable variance = 86.5%).

# 3. Results

## 3.1. AMF colonization rate of plant and AMF spore density in soil

The AMF infection structures in different plants are shown in Supplementary Figure 1. AMF within *A. argyi* roots produced numerous external hyphae, and vesicles formed at the tips of the external hyphae. AMF associated with *R. acetosa* and *C. abrotanoides* roots produced numerous internal hyphae and vesicles. AMF within *B. nivea* roots produced twining hyphae without vesicles. *R. acetosa* and *B. lindleyana* had relatively high AMF colonization rates (Figure 2A). There were significant differences in the colonization rates among S1 plants, with S1_Ra (sampling site_plant species) detecting the highest colonization rate (58.25 ± 6.41%). However, there were no significant differences among the sampling sites. The influence of different plant species ($F = 3.488$, $p = 0.022 < 0.050$) on the AMF colonization rate was greater than that of different sampling sites ($F = 1.301$, $p = 0.291$) (Supplementary Table 3).

There were 15 to 111 spores/g soil in the rhizosphere of different plants in different sampling sites (Figure 2B). The spore density in the rhizosphere soil of S1 was significantly higher than those of S0 and S2. The influence of different sampling sites ($F = 33.978$, $p < 0.001$) on the spore density was greater than that of different plant species ($F = 0.982$, $p = 0.436$) (Supplementary Table 3).

## 3.2. Overall sequencing results and AMF community composition

DNA was extracted from the 33 soil samples and amplified via PCR using the AML1 and AML2 primers in the first round and the AMV4.5NF and AMDGR primers in the second round. All of the reads assigned to AMF were aligned against the AMF sequences in the MaarjAM database. After leveling out according to the minimum number of sample sequences, 513,546 sequences were obtained. Overall, 268 AMF OTUs were detected, and a greater number of OTUs belonged to the Glomeraceae (88.27%, 193 OTUs, 453,321 sequences). Others belonged to the Diversisporaceae (6.09%, 16 OTUs, 31,293 sequences), Paraglomeraceae (3.81%, eight OTUs, 19,548 sequences), and Acaulosporaceae (1.47%, 14 OTUs, 7,571 sequences), while only a small number belonged to Gigasporaceae (0.22%, seven OTUs, 1,127 sequences) and Archaeosporaceae (0.03%, 11 OTUs, 160 sequences). In addition, 0.10% of all of the sequences were unclassified at the family

level. Detailed information on the OTUs in each sampling site is provided in Supplementary Table 4. The AMF community composition at the family level across different plants from the three investigated sampling sites was explored (Supplementary Figure 2). Glomeraceae was the dominant family in all of the groups of samples, and the relative abundance of each sample ranged from 78.41% in S1_Ra to 96.39% in S0_Ra.

The β-diversity of the AMF communities across different sampling sites and different plants based on the Bray–Curtis distance (Supplementary Figure 3). The total explanatory degree of the first two principal components of AMF community composition was 27.38%. The distribution of points in S0 was the most concentrated, and S2 was the most dispersed. The influence of different plants and different sampling sites on the AMF community was analyzed using PERMANOVA (Supplementary Table 5). The results showed that different plants ($R^2 = 0.163$, $p = 0.028 < 0.05$) and different sampling sites ($R^2 = 0.189$, $p < 0.001$) significantly affected the AMF community. The AMF communities between S0 and S1, S0 and S2, and S1 and S2 showed significant dissimilarities, which was confirmed by ANOSIM based on the Bray–Curtis distance ($p < 0.001$) (Supplementary Table 5). Among them, S1 and S2 had the lowest dissimilarity, followed by S0 and S1 (Supplementary Figure 3 and Supplementary Table 5).

The AMF richness, diversity, evenness, and coverage on the OTU level among the different sampling sites were estimated using the Sobs, Shannon, Shannoneven, and Coverage indexes (Figures 2C–F). Most rarefaction curves tended to saturate (Supplementary Figure 4). As shown in Figure 2, the Sobs index of different sampling sites indicated no significant differences in the richness of S0 and S1, but they were both higher than those of S2, and S0_Aa and S1_Aa had significantly higher richness than S2_Ra. The order of the Shannon index values among the three sampling sites was S0 > S1 > S2, and the diversity of S0 and S1_Aa was significantly higher than S2_Aa and S2_Ra. The Shannoneven index of S0 was higher than that of S1 and S2. The influence of different sampling sites ($F = 6.041$, $p = 0.007 < 0.010$ for Sobs; $F = 8.198$, $p = 0.002 < 0.010$ for Shannon; $F = 5.987$, $p = 0.008 < 0.010$ for Shannoneven) on the AMF richness, diversity, and evenness was greater than that of different plant species ($F = 0.593$, $p = 0.671$ for Sobs; $F = 0.912$, $p = 0.468$ for Shannon; $F = 1.153$, $p = 0.356$ for Shannoneven) (Supplementary Table 3).

A heat tree was used to compare differences in AMF community composition between sampling sites (Figure 3). Several species of *Glomus* were enriched in S0. Paraglomerales and Acaulosporaceae were enriched in S1. With the increase of Sb and As concentrations at the sampling sites, the Diversisporaceae genus *Glomus* was gradually enriched.

## 3.3. Correlation analysis between AMF community composition and soil properties

To eliminate multicollinearity, soil properties with VIF > 10 were screened before CCA analysis. The VIF values of the retained soil properties are shown in Supplementary Table 6. CCA was employed to determine the most significant soil properties that shaped the AMF community composition in three sampling sites
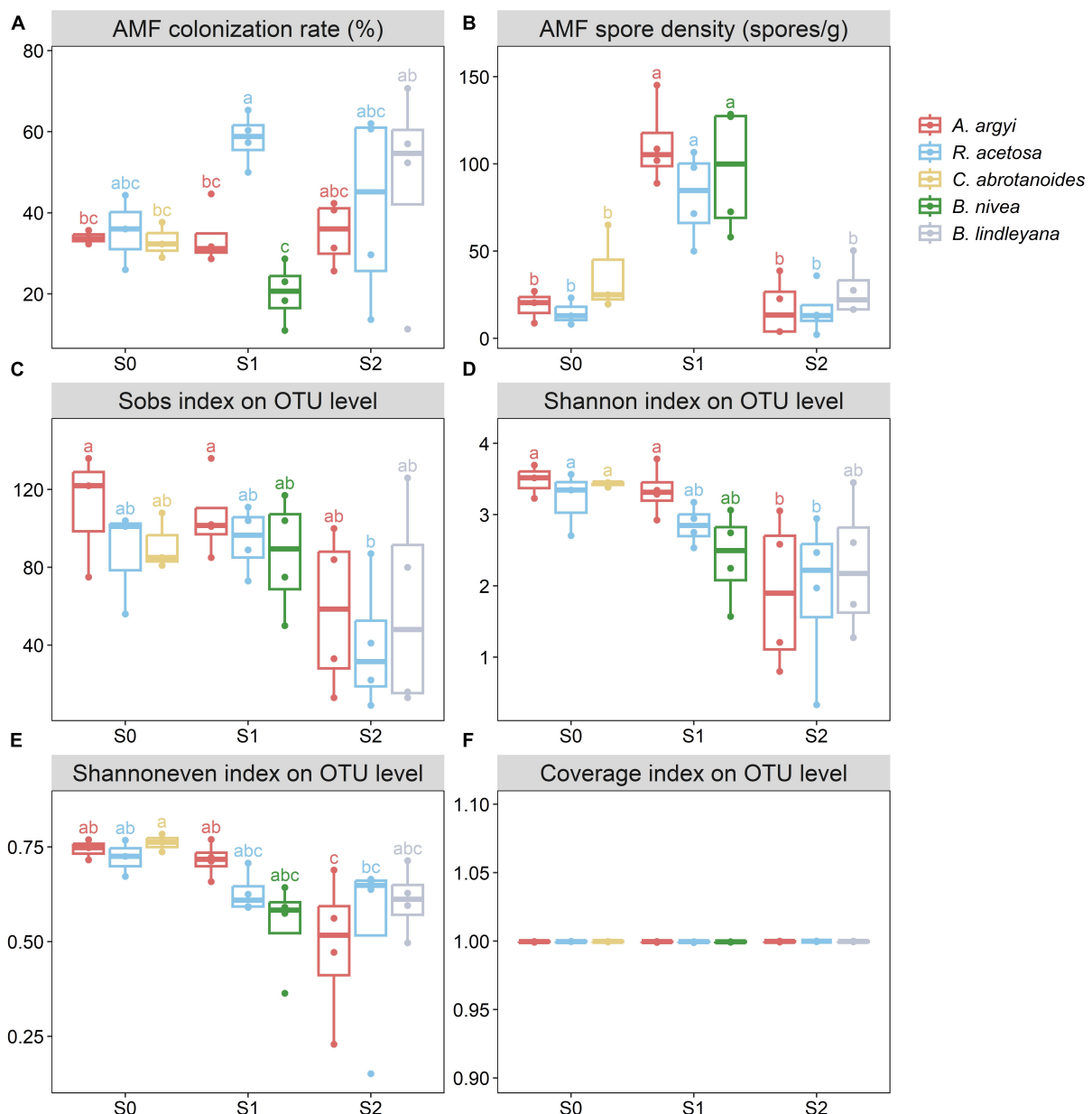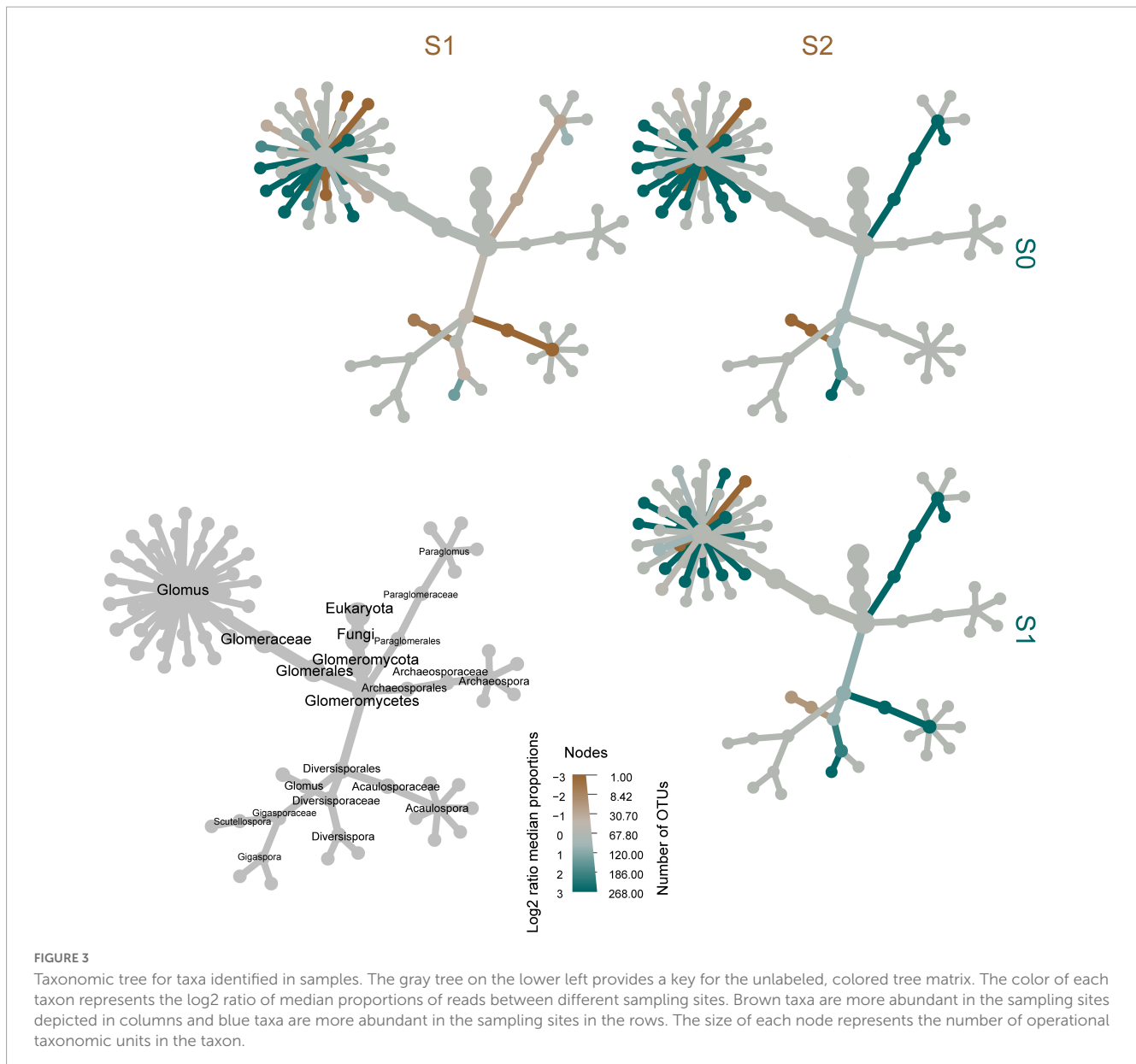
FIGURE 2
Arbuscular mycorrhizal fungi (AMF) colonization rate **(A)**, spore density **(B)**, and the Sobs **(C)**, Shannon **(D)**, Shannoneven **(E)**, and Coverage **(F)** indexes of different plants in different sampling sites. The line in the box represents the median value, box boundaries indicate values in the 25−75th percentile range, and whiskers indicate the 95% confidence intervals. Different letters indicate significant differences at $p < 0.05$. The absence of the same letter labels between any two boxes indicates that there is a significant difference.

using retained soil properties (**Figure 4A**). All of the variables explained 33.75% of the variation in the AMF communities, and only DTPA-As did not affect AMF community composition (**Supplementary Table 7**). In addition, AN, AK, TOC, pH, TCa, TSb, and TAs extremely significantly affected the community composition of AMF. According to the results of CCA, the soil properties that had a significant impact on the AMF community composition were divided into three groups, namely soil nutrients (including AN, AK, and TOC), heavy metals (including TAs, TSb, and DTPA-Sb), and pH and TCa. Then, VPA was conducted to compare the effects of soil nutrients, heavy metals, and pH and TCa on the AMF community composition (**Figure 4B**). Totals of 15.36,

5.80, and 1.50% of the variation could be assigned to soil nutrients, heavy metals, and pH and TCa independently.

A Mantel test was used to calculate the correlation between soil properties and the AMF colonization rate, spore density, and the Sobs, Shannon, and Shannoneven indexes (**Figure 5A**), and between soil properties and AMF families (**Figure 5B**). TAs was significantly negatively correlated with AN, but positively correlated with AP, EC, TCa, TSb, and DTPA-Sb. TSb was significantly positively correlated with AP, EC, DTPA-Sb, and TAs (**Figure 5**). The AMF colonization rate correlated with AP ($R = 0.166$, $p = 0.034$) and TSb ($R = 0.220$, $p = 0.015$); spore density was correlated with AN ($R = 0.401$, $p = 0.003$), AK ($R = 0.337$,

**FIGURE 3**
Taxonomic tree for taxa identified in samples. The gray tree on the lower left provides a key for the unlabeled, colored tree matrix. The color of each taxon represents the log2 ratio of median proportions of reads between different sampling sites. Brown taxa are more abundant in the sampling sites depicted in columns and blue taxa are more abundant in the sampling sites in the rows. The size of each node represents the number of operational taxonomic units in the taxon.

$p = 0.004$), and TOC ($R = 0.230$, $p = 0.043$); the Sobs index was correlated with AP ($R = 0.412$, $p = 0.001$), EC ($R = 0.461$, $p = 0.001$), TSb ($R = 0.185$, $p = 0.028$), and TAs ($R = 0.339$, $p = 0.003$); the Shannon index was correlated with AP ($R = 0.462$, $p = 0.001$), EC ($R = 0.377$, $p = 0.003$), TCa ($R = 0.152$, $p = 0.050$) TSb ($R = 0.279$, $p = 0.017$), DTPA-Sb ($R = 0.254$, $p = 0.034$), and TAs ($R = 0.339$, $p = 0.003$); and the Shannoneven index was correlated with AP ($R = 0.318$, $p = 0.007$) and TAs ($R = 0.214$, $p = 0.039$) (**Figure 5A**). Diversisporaceae was correlated with EC ($R = 0.240$, $p = 0.042$); Glomeraceae was correlated with AP ($R = 0.383$, $p = 0.003$), EC ($R = 0.293$, $p = 0.016$), TSb ($R = 0.416$, $p = 0.007$), DTPA-Sb ($R = 0.321$, $p = 0.034$), TAs ($R = 0.285$, $p = 0.017$), and DTPA-As ($R = 0.257$, $p = 0.038$); Paraglomeraceae was correlated with AK ($R = 0.330$, $p = 0.023$); and unclassified Glomeromycetes was correlated with AN ($R = 0.436$, $p = 0.006$) and TOC ($R = 0.731$, $p = 0.013$) (**Figure 5B**). The Pearson correlation coefficient showed that the AMF colonization rate was positively correlated with AP; spore density was extremely significantly positively correlated

with the AN, AK, and TOC and extremely significantly negatively correlated with EC; the Sobs index was positively correlated with AN and negatively correlated with AP, EC, TSb, DTPA-Sb, and TAs; and the Shannon and Shannoneven indexes were negatively correlated with AP, EC, TCa, TSb, DTPA-Sb, and TAs (**Supplementary Table 8**).

Two-factor network analysis result showed that a total of 39 OTUs were correlated with TAs, indicating that TAs was particularly important for the distribution of the AMF community composition, followed by AN (37 OTUs), TCa (30 OTUs), EC (29 OTUs), pH (28 OTUs), TSb (24 OTUs), AK (22 OTUs) and TOC (22 OTUs) (**Figure 6**). A correlation heatmap was used to demonstrate the correlation between soil properties and AMF richness at the family level (**Supplementary Figure 5**). The richness of Diversisporaceae was positively correlated with the TSb and TAs. AMF that was unclassified at the family level was positively correlated with DTPA-Sb and DTPA-As.
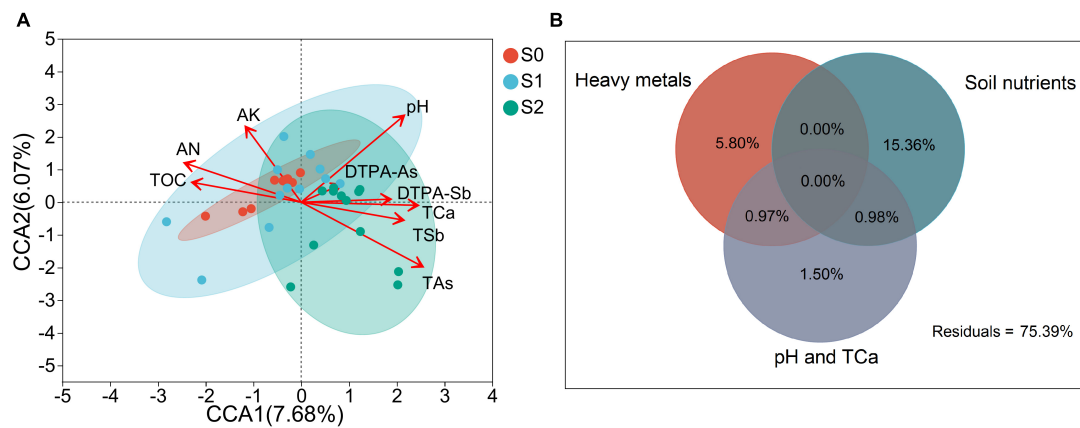
FIGURE 4

Canonical correspondence analysis (CCA) ordination plots of communities of arbuscular mycorrhizal fungi (AMF) from three sampling sites **(A)** and variation partition analysis (VPA) of the effects of three groups of soil properties on the community composition of arbuscular mycorrhizal fungi **(B)**. The red arrows represent soil properties. The arrow length indicates the degree of influence of soil properties on the AMF community composition. The angles between the arrows of soil properties represent a positive or negative correlation. The circles represent soil samples from different sites. AN, available nitrogen; AK, available potassium; TOC, total organic carbon; TSb, total antimony; DTPA-Sb, diethylenetriamine pentaacetic acid-extractable antimony; TAs, total arsenic; DTPA-As, diethylenetriamine pentaacetic acid-extractable arsenic; TCa, total calcium.
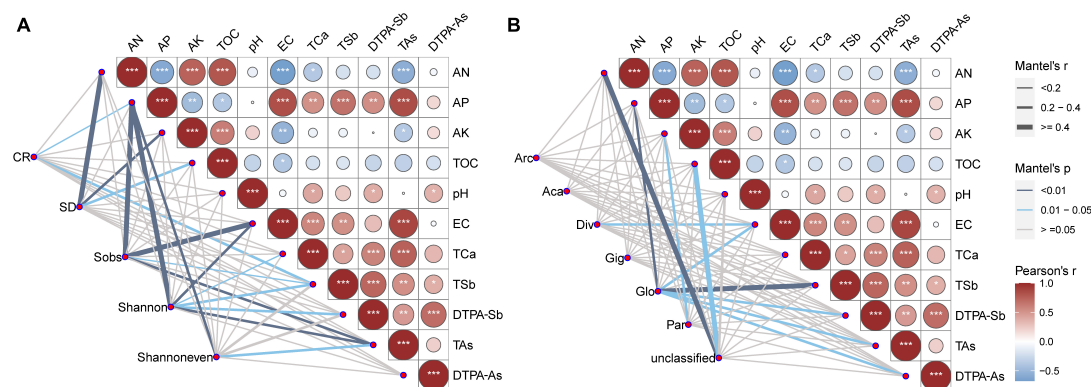


FIGURE 5

Correlation analysis between soil properties and the AMF colonization rate, spore density, and the Sobs, Shannon, and Shannoneven indexes **(A)**, and between soil properties and AMF families **(B)**. Pairwise comparisons of environmental factors are shown with a color gradient denoting the Pearson correlation coefficients. The edge width corresponds to Mantel's R statistic for the corresponding distance correlations, and the edge color denotes the statistical significance. AN, available nitrogen; AP, available phosphorus; AK, available potassium; TOC, total organic carbon; TSb, total antimony; DTPA-Sb, diethylenetriamine pentaacetic acid-extractable antimony; TAs, total arsenic; DTPA-As, diethylenetriamine pentaacetic acid-extractable arsenic; EC, electrical conductivity; TCa, total calcium; CR, AMF colonization rate; SD, spore density; Arc, Archaeosporaceae; Aca, Acaulosporaceae; Div, Diversisporaceae; Gig, Gigasporaceae; Glo, Glomeraceae; Par, Paraglomeraceae; unclassified, unclassified Glomeromycetes. *$p < 0.05$; **$p < 0.01$; ***$p < 0.001$.

## 3.4. Integrated responses of the effects of soil properties on AMF richness and diversity

The SEM was employed to investigate the integrated responses of the effects of soil properties on AMF richness and diversity (Figure 7). The final model was found to be a good fit to the data ($\chi^2 = 6.7$, $p = 0.878$; CFI = 1.00, GFI = 0.95, RMSEA < 0.001), accounting for 48, 43, and 13% of the variation in the AMF richness and diversity, the spore density, and the colonization rate, respectively. TAs had a significant direct effect on AMF richness and diversity ($\lambda = -0.96$), but the direct effect of TSb on AMF richness and diversity was not significant ($\lambda = -0.21$). In addition to the strong direct correlation between TSb and TAs ($\lambda = 0.51$),

there is also a strong direct correlation between TAs and TCa ($\lambda = 0.77$). Moreover, TAs directly affected the content of soil nutrients ($\lambda = -0.53$) initially and then indirectly affected AMF spore density ($\lambda = 0.58$).

# 4. Discussion

## 4.1. Plant species but not soil properties influenced AMF colonization rate

Arbuscular mycorrhizal fungi (AMF) can colonize the majority of terrestrial plants and form mycorrhizal structures (Kohout et al., 2014; Jiang et al., 2020; Guzman et al., 2021), even
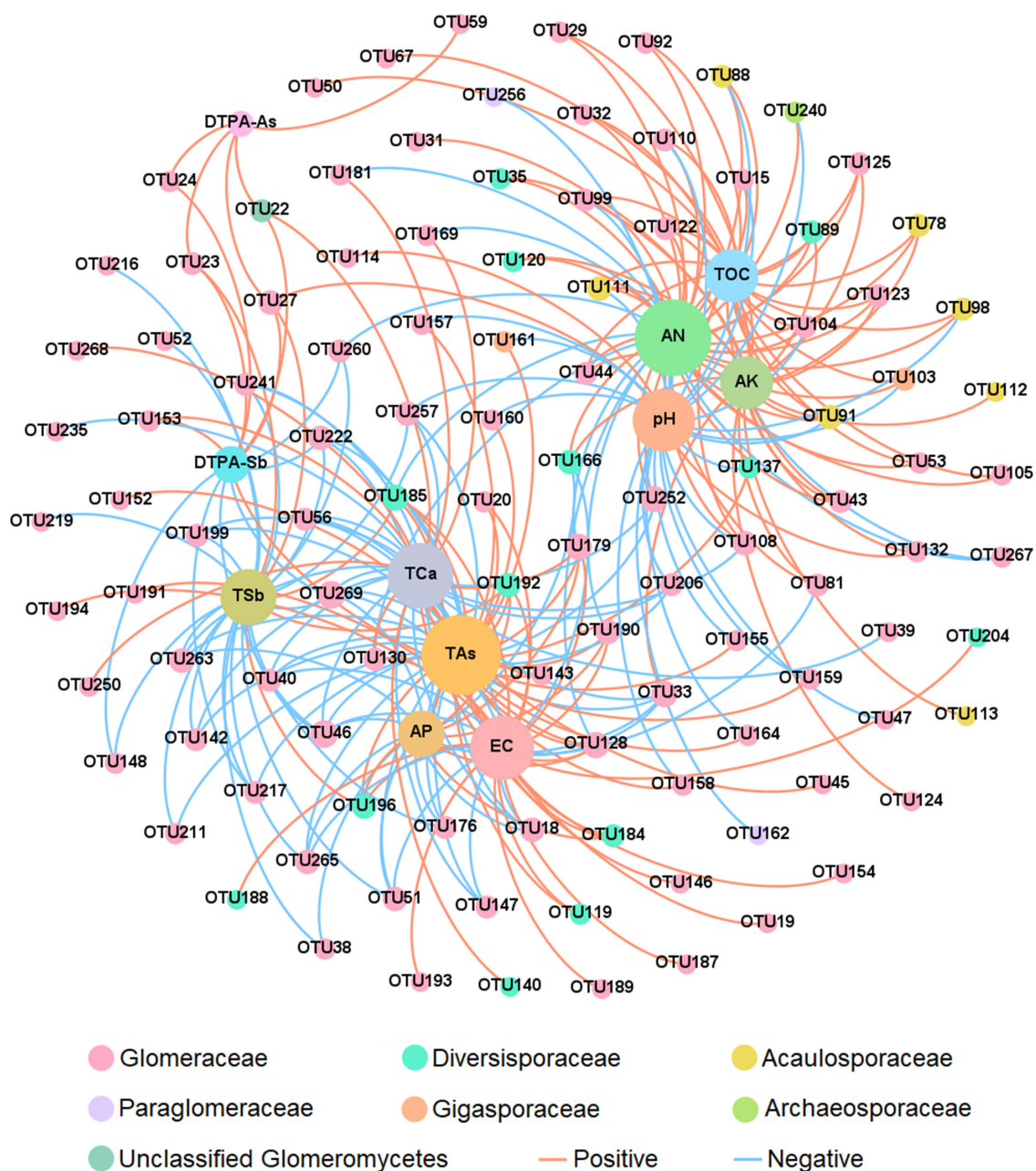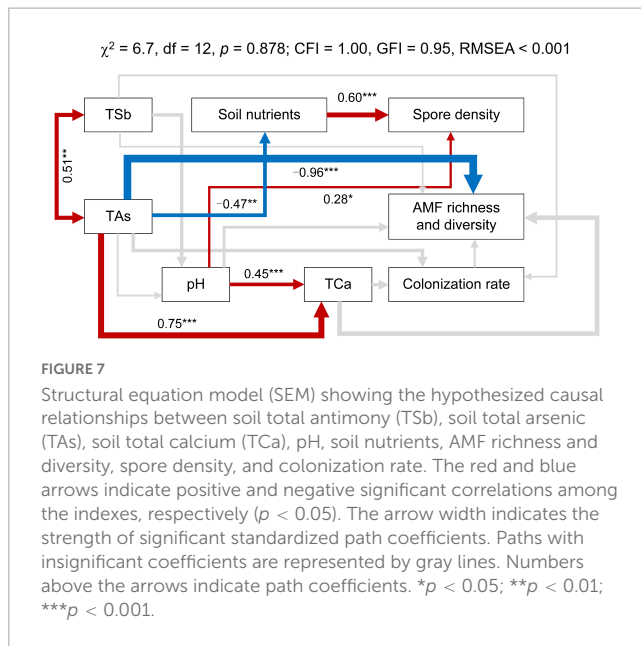
FIGURE 6
Two-factor network analysis of the association between arbuscular mycorrhizal fungi (AMF) OTUs and environmental factors. The different colors of the species represent the family they belong to. Lines between the points represent a significant correlation ($p < 0.05$) as shown by the Pearson correlation coefficient. Operational taxonomic units (OTUs) were the top 200 species in terms of abundance. AN, available nitrogen; AP, available phosphorus; AK, available potassium; TOC, total organic carbon; TSb, total antimony; DTPA-Sb, diethylenetriamine pentaacetic acid-extractable antimony; TAs, total arsenic; DTPA-As, diethylenetriamine pentaacetic acid-extractable arsenic; EC, electrical conductivity; TCa, total calcium.

in heavy metal-contaminated areas (Sanchez-Castro et al., 2017; Zhan et al., 2019; Riaz et al., 2021). In this study, the roots and rhizosphere soils of five different plants, namely *A. argyi*, *R. acetosa*, *C. abrotanoides*, *B. nivea*, and *B. lindleyana* were collected from areas with different levels of Sb and As contamination, and obvious mycorrhizal infection structures were detected in the roots of these plants (**Supplementary Figure 1**).

The results showed that the infection structures and colonization rates of these five plants were different (**Figure 2A**). Multi-way ANOVA analysis showed that the influence of different

host plant species on AMF colonization rates was greater than the differences in soil properties caused by spatial heterogeneity (**Supplementary Table 3**), which was consistent with the results of previous studies (Spruyt et al., 2014; Sanchez-Castro et al., 2017; de Fatima Pedroso et al., 2018). Some studies have suggested that the host plant species is a decisive factor in the colonization of particular AMF species (Teodoro et al., 2020). This may be due to differences in root structure or plant nutrient requirements (Karanika et al., 2008). It was interesting to find that Sb and As contamination did not significantly affect the AMF colonization

FIGURE 7
Structural equation model (SEM) showing the hypothesized causal relationships between soil total antimony (TSb), soil total arsenic (TAs), soil total calcium (TCa), pH, soil nutrients, AMF richness and diversity, spore density, and colonization rate. The red and blue arrows indicate positive and negative significant correlations among the indexes, respectively ($p < 0.05$). The arrow width indicates the strength of significant standardized path coefficients. Paths with insignificant coefficients are represented by gray lines. Numbers above the arrows indicate path coefficients. *$p < 0.05$; **$p < 0.01$; ***$p < 0.001$.

rates (**Figure 5A**), which was different from the results of Yang et al. (2016). However, a large number of previous studies were consistent with the results of the present study (Ruotsalainen et al., 2007; Schneider et al., 2016). Teodoro et al. (2020) indicated that differences in the frequency and intensity of colonization were found for different plant species, but that the concentrations of Zn, Pb, As, and Cd in rhizospheres and plants were poorly correlated with AMF colonization. Malcová et al. (2003) conducted a cultivation experiment and found that the addition of Pb at different concentrations did not change the percentage of root colonization.

## 4.2. Spore density was not directly affected by soil Sb and As content

The AMF spore density varied greatly in different sampling sites (**Figure 2B**). Unlike the colonization rates, the AMF spore density was mainly affected by soil properties rather than the host plants (**Supplementary Table 3**), which was consistent with previous studies (Birhane et al., 2017; Coutinho et al., 2019; Guo et al., 2020). However, the results showed that Sb and As content in soil was still not the main factor affecting the AMF spore density. At present, there are different opinions about the effect of heavy metals on AMF spore density, including a positive correlation (Krishnamoorthy et al., 2015), a negative correlation (Zarei et al., 2008, 2010; Schneider et al., 2013), and no correlation (Yang et al., 2015). This phenomenon may be caused by the different sensitivities of different AMFs to different heavy metals (Pawlowska and Charvat, 2004). In addition, the effects of heavy metals on the sporulation process of AMF may depend on other environmental factors (Yang et al., 2015). In this study, it was found that the AMF spore density was positively correlated with AN, and TOC (**Figures 5A**, **7**), which is consistent with the results of previous studies (Bhat et al., 2014; de Araujo Pereira et al., 2018; Amir et al., 2022). It is generally believed that the AMF spore density

is positively correlated with soil nitrogen and organic matter when the soil nutrient content is low (Moradi et al., 2017). For example, Zhang et al. (2021) indicated that increasing the C:N ratio favored sporulation. Another reason for this phenomenon may be related to the glomalin secreted by AMF spore, which is one of the major sources of soil organic carbon and nitrogen (Guo et al., 2020). However, TAs most likely affects soil spore density by affecting soil N, TOC, and other nutrients. In the present study, TAs was found to be negatively correlated with soil AN, AK, and TOC (**Figures 5**, **7**). Previous studies have shown that As contamination can significantly reduce soil microbial biomass nitrogen and microbial biomass carbon, which are important sources of soil nitrogen and organic carbon (Ghosh et al., 2004). In addition, a large number of studies have confirmed that soil As pollution reduces soil biodiversity (Yu et al., 2021; Jia et al., 2022) and then affects the cycling of C, N, and other elements in the soil.

## 4.3. As had a stronger effect on AMF community composition than Sb

It was found that the AMF community composition was significantly affected by different plant species and sampling sites (**Supplementary Figure 3** and **Supplementary Table 5**). There was no significant difference in AMF community composition between *A. argyi* and *R. acetosa* rhizosphere soils, the differences were mainly in the rhizosphere soils of *C. abrotanoides*, *B. nivea*, and *B. lindleyana*. This difference may have been because these plants were located at different sampling sites, and the differences in the AMF community composition between sampling sites led to the differences in the AMF community composition in these plant rhizosphere soils. In this study, the AMF community composition was different among sampling sites (**Supplementary Figure 3** and **Supplementary Table 5**). Because all of the sampling sites were located in Qinglong County, Qianxinan Buyei and Miao Autonomous Prefecture, Guizhou Province, the differences in climate between the sampling sites could be ignored. Therefore, such differences in AMF community composition were more likely to be related to differences in soil properties. Many studies have demonstrated that soil properties can significantly affect the AMF community composition (Wu et al., 2020; Silva et al., 2022). The Sobs, Shannon, Shannoneven, and Coverage indexes were used to evaluate the AMF richness, diversity, evenness, and coverage at different sampling sites, respectively (**Figures 2C–F**). The results showed that the order of AMF richness and diversity of the three sampling sites was S0 > S1 > S2. Multi-way ANOVA analysis showed that the variation of soil properties was the dominant factor influencing AMF diversity (**Supplementary Table 3**), which was consistent with the results on spore density (**Supplementary Table 3**) and AMF community composition (**Supplementary Table 5**). Previous studies have also supported these phenomena (Faggioli et al., 2019; Faghihinia et al., 2021).

To further understand which soil properties were the main influencing factors for AMF community composition, CCA analysis was performed after multivariate collinear screening (**Figure 4** and **Supplementary Table 6**). CCA analysis showed that eight soil properties had significant effects on the AMF community composition, namely AN, AK, TOC, pH, TCa, TSb,

DTPA-Sb, and TAs. It should be noted that AP and EC were removed due to multicollinearity with other environmental factors (**Supplementary Table 6**). The Pearson correlation coefficient showed that there was an extremely strong correlation between AP, EC, and TAs (Pearson's $R > 0.8$) (**Supplementary Table 9**), and the effect of AP and EC on the AMF community composition could be approximated by TAs. All the soil properties that significantly affected AMF community composition were divided into three groups according to their attributes, namely soil nutrients, heavy metals, and pH and TCa. VPA analysis was used to compare the effects of these three groups of soil properties on the AMF community composition (**Figure 4B**). The results showed that soil nutrients were the most important factors affecting the AMF community composition. The effects of soil nutrient content (Yan K. et al., 2021; Yan T. et al., 2021; Emery et al., 2022), pH (Van Geel et al., 2018; Xiao et al., 2022), and heavy metal content (Zarei et al., 2010; Faggioli et al., 2019) on the AMF community composition have been extensively demonstrated. However, few studies have discussed which group of soil properties has a greater impact on AMF community composition. Stefanowicz et al. (2020) indicated that although heavy metal pollution was a meaningful agent shaping soil microbial communities, the toxic effect of heavy metals was weaker than the organic matter content, which was consistent with the present results. In contrast, Zhang et al. (2019) found that the soil pH and EC were more important than the available N, P, and K drivers of the variation of AMF diversity in saline-sodic soils, which was different from the results of this study. This may be due to the complex interrelationship between soil properties, groups, models, and soil types will affect the analysis results. Understanding the dominant factors that induce changes in the AMF community composition is of great practical significance for the design of AMF application techniques.

A Mantel test was used to investigate the effects of soil properties on the richness, diversity, and evenness of AMF, AP, EC, TCa, TSb, DTPA-Sb, and TAs, which significantly affected the AMF richness and diversity (**Figure 5**). Thirty-nine and 24 OTUs were closely related to TAs and TSb (**Figure 6**), respectively, thus indicating that both TSb and TAs greatly affected the AMF community composition, but TAs had a greater effect than TSb. As expected, both TAs and TSb were significantly negatively correlated with AMF richness and diversity (**Supplementary Table 8**), which confirmed the majority view that heavy metal pollution would reduce AMF richness and diversity (Faggioli et al., 2019; Parvin et al., 2019). Excessive heavy metal concentrations are toxic to most AMFs. Only AMFs that exhibit strong heavy metal tolerances can survive, which reduces AMF diversity (Pawlowska and Charvat, 2004; Faggioli et al., 2019). Although Schneider et al. (2013) concluded that As contamination reduced the AMF species richness in an investigation of the AMF community composition in a gold mining area in Minas Gerais State, Brazil, they did not systematically analyze the correlation between soil As content and other properties and AMF diversity. The results of the present study provide direct evidence for this conclusion. Wei et al. (2015a) also investigated the AMF community composition in an Sb mining area and preliminarily concluded that Sb dominated the distribution of the AMF community composition. However, their study only considered the effects of Sb, P, N, pH, and organic matter on the AMF community composition, and it did not take the As content into account. Sb and As often co-occur in landscapes

impacted by mining activities (Johnston et al., 2020); therefore, the influence of As pollution in Sb mining areas cannot be ignored. The present study provides direct evidence that although Sb has a significant effect on the AMF community composition, As is the more important factor affecting the AMF community composition in Sb and As mining areas.

It is worth noting that there was a strong positive correlation between AP, TAs, and EC (**Figure 5** and **Supplementary Table 9**). AP has been widely confirmed to be an important factor affecting AMF community composition (Zarei et al., 2010). There is competitive adsorption between As and P in soil (Gunes et al., 2008). P can be desorbed by As due to a mass action effect of high As concentrations (Anawar et al., 2018), and it can then improve the availability of P. Numerous studies have shown that interactions between As and P in the soil can significantly affect the availability of As and P (Wu et al., 2022). There are reciprocal reward mechanisms between AMF and host plants (Kiers et al., 2011), wherein AMF can provide mineral nutrients to host plants (especially P) and other benefits, including protection against biotic and abiotic stresses (Smith et al., 2009; Huang et al., 2019). In exchange, plants supply AMF with carbohydrates, which are essential and necessary for fungal survival and growth (Parniske, 2008). High soil P content allows plants to take up P without resorting to mycorrhizal symbionts, which in turn reduces the supply of carbohydrates from the host plants to the symbiotic AMF (Johnson et al., 2013). Therefore, this study indicated that the effect of soil As on AMF community composition cannot be simply attributed to the toxic effect of As on AMF, but should be caused by the joint effect of As and P.

In addition, the present study found that AMF richness was positively correlated with AN, while AMF richness and diversity were negatively correlated with TCa (**Supplementary Table 8**). Some genera of AMF need to obtain more organic acids from microbial metabolism when microbial biomass increases, thus leading to a significant correlation between the AMF richness and microbial biomass N (Xiao D. et al., 2019). Xiao et al. (2022) found that the decreases in microbial motility caused by high Ca resulted in the decline of some AMF groups and the selection of certain AMF species (Tang et al., 2019), leading to a significantly negative correlation between the AMF diversity and Ca content.

Glomeraceae was detected as the dominant family in all of the groups of samples in this study (**Supplementary Figure 2**). Numerous studies have suggested that Glomeraceae exhibits strong ecological adaptability and it is the dominant family in areas under heavy metal stress (Zarei et al., 2008; Long et al., 2010; Yang et al., 2015; Sanchez-Castro et al., 2017; Faggioli et al., 2019), including areas contaminated with Sb (Wei et al., 2015a) or As (Parvin et al., 2019). One possible reason is that Glomeraceae can repair damaged hyphae in stressful environments, which helps to improve the ability of these fungi to adapt to environmental stresses (de la Providencia et al., 2005; Huang et al., 2019). Another reason is that plants harbor Glomeraceae that can benefit their growth and improve their competitiveness under specific environmental conditions (Wei et al., 2015b; Huang et al., 2019), thereby promoting the dominance of Glomeraceae in soil ecosystems. Other studies suggest that the predominant detection of Glomeraceae might be explained by their high sporulation rate (Sanchez-Castro et al., 2017). Previous studies have demonstrated that Glomeraceae can form beneficial symbiotic relationships

with various plants, and enhance the efficiency of the ecological restoration of heavy metal-contaminated soil by promoting the growth or heavy metal absorption of plants (Riaz et al., 2021). Glomeraceae is widely distributed, even in Sb- and As-polluted soil, and it seems to be a potential option to promote ecological remediation efficacy in Sb- and As-contaminated areas. In addition, the present study found that TSb and TAs significantly affected the community structure of the Glomeraceae (Figures 3, 5B, 6). This phenomenon indicates that even AMFs of the same family have different sensitivities to heavy metals (Faggioli et al., 2019). Interestingly, the study found that the richness of Diversisporaceae was positively correlated with the TSb and TAs (Figure 3 and Supplementary Figure 5). Parvin et al. (2019) found three AMF families that predominated in most As-contaminated soils, namely Glomeraceae, Claroideoglomeraceae, and Diversisporaceae. The results of this study supported this research phenomenon and directly confirmed that there was a positive linear correlation between Diversisporaceae and soil TSb and TAs. This finding may be due to the high Sb and As tolerance of Diversisporaceae itself, leading to its high relative abundance in soil with high concentrations of Sb and As.

The SEM demonstrated the relationship between soil environmental factors and the AMF richness and diversity, spore density, and the colonization rate in the system examined in this study (Figure 7). It has been well documented that Sb and As often co-exist and co-contaminate adjacent regions (Okkenhaug et al., 2012; Li Y. et al., 2021). Therefore, TSb and TAs are positively correlated, and together they negatively affect AMF richness and diversity, with TAs having an extremely significant effect on AMF richness and diversity. There was a negative correlation between soil nutrients (mainly AN, AK, and TOC) and TAs. High levels of As contamination decrease soil nutrition cycling by inhibiting the growth of soil animals, plants, and microbes (Jiao et al., 2016). In addition, Yu et al. (2021) found that high Sb and As stress inhibited the microbial carbon mineralization and nitrification processes in the plant rhizosphere soils and further reduced soil enzymatic activities, carbon mineralization, and nitrification potential, of which the disruption caused by As was more obvious. The positive relationship between soil nutrients and spore density was mainly because soil C and N promoted AMF sporulation (Zhang et al., 2021).

## 5. Conclusion

The present study identified the AMF community composition and its main influencing factors in Sb- and As-contaminated areas. Glomeraceae was the dominant family in Sb and As mining areas. In Sb- and As-polluted areas, the affinity between AMF and plants is mainly affected by plant species, and less affected by soil Sb and As content. Spore density is mainly affected by soil nutrients, such as AN, AK, and TOC, but soil TAs contamination may be important environmental property sleading to low soil nutrient content. The effect of soil nutrients on AMF community composition was also greater than that of TSb and TAs contamination. However, soil contamination with Sb and As also had a significant effect on AMF community composition, with the effect of TAs being significantly greater than that of TSb. The effect of TAs on AMF

community composition cannot be attributed to the toxic effect of As on AMF alone, and the interaction of As and P is also an important reason for the reduction of soil AMF richness and diversity. Therefore, the potential impact of As on the effective application of mycorrhizal technology should be further considered when this technology is applied to the ecological restoration of Sb- and As-contaminated areas.

## Data availability statement

The datasets presented in this study can be found in online repositories. The names of the repository/repositories and accession number(s) can be found in the article/Supplementary material.

## Author contributions

YM: investigation, data curation, methodology, software, visualization, and writing—original draft preparation. XRL, MZ, KC, CD, and XML: investigation. CX, NJ, FW, HS, and XSL: manuscript revision. YW: conceptualization, data curation, manuscript revision, and funding acquisition. All authors contributed to the article and approved the submitted version.

## Funding

## Conflict of interest

The authors declare that the research was conducted in the absence of any commercial or financial relationships that could be construed as a potential conflict of interest.

## Publisher's note

## Supplementary material

The Supplementary Material for this article can be found online at: https://www.frontiersin.org/articles/10.3389/fmicb.2023.1189400/full#supplementary-material

# References

Alam, M. Z., Hoque, M. A., Ahammed, G. J., and Carpenter-Boggs, L. (2019). Arbuscular mycorrhizal fungi reduce arsenic uptake and improve plant growth in *Lens culinaris*. *PLoS One* 14:e0211441. doi: 10.1371/journal.pone.0211441

Amato, K. R., Yeoman, C. J., Kent, A., Righini, N., Carbonero, F., Estrada, A., et al. (2013). Habitat degradation impacts black howler monkey (*Alouatta pigra*) gastrointestinal microbiomes. *ISME J.* 7, 1344–1353. doi: 10.1038/ismej.2013.16

Amir, H., Bordez, L., Cavaloc, Y., Jourand, P., Ducousso, M., and Juillot, F. (2022). Effects of ultramafic topsoil stockpiling during mine activities on its microbial diversity and other microbiological and physicochemical characteristics. *Ecol. Eng.* 177:106563. doi: 10.1016/j.ecoleng.2022.106563

Anawar, H. M., Freitas, M. C., Canha, N., and Santa Regina, I. (2011). Arsenic, antimony, and other trace element contamination in a mine tailings affected area and uptake by tolerant plant species. *Environ. Geochem. Health* 33, 353–362. doi: 10.1007/s10653-011-9378-2

Anawar, H. M., Rengel, Z., Damon, P., and Tibbett, M. (2018). Arsenic-phosphorus interactions in the soil-plant-microbe system: Dynamics of uptake, suppression and toxicity to plants. *Environ. Pollut.* 233, 1003–1012. doi: 10.1016/j.envpol.2017.09.098

Bhat, B. A., Sheikh, M. A., and Tiwari, A. (2014). Impact of various edaphic factors on AMF spore population and diversity in *Catharanthus roseus* at Gwalior. *Int. J. Plant Sci.* 9, 1–6.

Bi, Y., Zhang, J., Song, Z., Wang, Z., Qiu, L., Hu, J., et al. (2019). Arbuscular mycorrhizal fungi alleviate root damage stress induced by simulated coal mining subsidence ground fissures. *Sci. Total Environ.* 652, 398–405. doi: 10.1016/j.scitotenv.2018.10.249

Birhane, E., Fatumah, N., Gidey, K., Zenebe, A., and Mohammed, S. (2017). Vegetation cover density and disturbance affected arbuscular mycorrhiza fungi spore density and root colonization in a dry Afromontane forest, northern Ethiopia. *J. For. Res.* 29, 675–686. doi: 10.1007/s11676-017-0493-5

Chang, C., Li, F., Wang, Q., Hu, M., Du, Y., Zhang, X., et al. (2022). Bioavailability of antimony and arsenic in a flowering cabbage-soil system: Controlling factors and interactive effect. *Sci. Total Environ.* 815:152920. doi: 10.1016/j.scitotenv.2022.152920

Coutinho, E. S., Barbosa, M., Beiroz, W., Mescolotti, D. L. C., Bonfim, J. A., Louro Berbara, R. L., et al. (2019). Soil constraints for arbuscular mycorrhizal fungi spore community in degraded sites of rupestrian grassland: Implications for restoration. *Eur. J. Soil Biol.* 90, 51–57. doi: 10.1016/j.ejsobi.2018.12.003

de Araujo Pereira, A. P., Santana, M. C., Bonfim, J. A., de Lourdes Mescolotti, D., and Cardoso, E. J. B. N. (2018). Digging deeper to study the distribution of mycorrhizal arbuscular fungi along the soil profile in pure and mixed *Eucalyptus grandis* and *Acacia mangium* plantations. *Appl. Soil Ecol.* 128, 1–11. doi: 10.1016/j.apsoil.2018.03.015

de Fatima Pedroso, D., Barbosa, M. V., Dos Santos, J. V., Pinto, F. A., Siqueira, J. O., and Carneiro, M. A. C. (2018). Arbuscular mycorrhizal fungi favor the initial growth of *Acacia mangium*, *Sorghum bicolor*, and *Urochloa brizantha* in soil contaminated with Zn, Cu, Pb, and Cd. *Bull. Environ. Contam. Toxicol.* 101, 386–391. doi: 10.1007/s00128-018-2405-6

de la Providencia, I. E., de Souza, F. A., Fernandez, F., Delmas, N. S., and Declerck, S. (2005). Arbuscular mycorrhizal fungi reveal distinct patterns of anastomosis formation and hyphal healing mechanisms between different phylogenic groups. *New Phytol.* 165, 261–271. doi: 10.1111/j.1469-8137.2004.01236.x

Emery, S. M., Bell-Dereske, L., Stahlheber, K. A., and Gross, K. L. (2022). Arbuscular mycorrhizal fungal community responses to drought and nitrogen fertilization in switchgrass stands. *Appl. Soil Ecol.* 169:104218. doi: 10.1016/j.apsoil.2021.104218

Faggioli, V., Menoyo, E., Geml, J., Kemppainen, M., Pardo, A., Salazar, M. J., et al. (2019). Soil lead pollution modifies the structure of arbuscular mycorrhizal fungal communities. *Mycorrhiza* 29, 363–373. doi: 10.1007/s00572-019-00895-1

Faghihinia, M., Zou, Y., Bai, Y., Dudas, M., Marrs, R., and Staddon, P. L. (2021). Grazing intensity rather than host plant's palatability shapes the community of arbuscular mycorrhizal fungi in a steppe grassland. *Microb. Ecol.* 84, 1062–1071. doi: 10.1007/s00248-021-01920-7

Foster, Z. S. L., Sharpton, T. J., and Grünwald, M. J. (2016). Metacoder: An R package for visualization and manipulation of community taxonomic diversity data. *PLoS Comput. Biol.* 13:e1005404. doi: 10.1371/journal.pcbi.1005404

Ghosh, A. K., Bhattacharyya, P., and Pal, R. (2004). Effect of arsenic contamination on microbial biomass and its activities in arsenic contaminated soils of Gangetic West Bengal India. *Environ. Int.* 30, 491–499. doi: 10.1016/j.envint.2003.10.002

Gu, H. H., Zhou, Z., Gao, Y. Q., Yuan, X. T., Ai, Y. J., Zhang, J. Y., et al. (2017). The influences of arbuscular mycorrhizal fungus on phytostabilization of lead/zinc tailings using four plant species. *Int. J. Phytoremediat.* 19, 739–745. doi: 10.1080/15226514.2017.1284751

Gunes, A., Pilbeam, D. J., and Inal, A. (2008). Effect of arsenic–phosphorus interaction on arsenic-induced oxidative stress in chickpea plants. *Plant Soil* 314, 211–220. doi: 10.1007/s11104-008-9719-9

Guo, Y., Chen, J., Tsolmon, B., He, A., Guo, J., Yang, J., et al. (2020). Effects of subsidence and transplanted trees on soil arbuscular mycorrhizal fungal diversity in a coal mining area of the Loess Plateau. *Glob. Ecol. Conserv.* 24:e01308. doi: 10.1016/j.gecco.2020.e01308

Guzman, A., Montes, M., Hutchins, L., DeLaCerda, G., Yang, P., Kakouridis, A., et al. (2021). Crop diversity enriches arbuscular mycorrhizal fungal communities in an intensive agricultural landscape. *New Phytol.* 231, 447–459. doi: 10.1111/nph.17306

Huang, Z., Zhao, F., Wang, M., Qi, K., Wu, J., and Zhang, S. (2019). Soil chemical properties and geographical distance exerted effects on arbuscular mycorrhizal fungal community composition in pear orchards in Jiangsu Province, China. *Appl. Soil Ecol.* 142, 18–24. doi: 10.1016/j.apsoil.2019.05.017

Jia, P., Li, F., Zhang, S., Wu, G., Wang, Y., and Li, J. (2022). Microbial community composition in the rhizosphere of *Pteris vittata* and its effects on arsenic phytoremediation under a natural arsenic contamination gradient. *Front. Microbiol.* 13:989272. doi: 10.3389/fmicb.2022.989272

Jiang, S., Hu, X., Kang, Y., Xie, C., An, X., Dong, C., et al. (2020). Arbuscular mycorrhizal fungal communities in the rhizospheric soil of litchi and mango orchards as affected by geographic distance, soil properties and manure input. *Appl. Soil Ecol.* 152:103593. doi: 10.1016/j.apsoil.2020.103593

Jiao, S., Liu, Z., Lin, Y., Yang, J., Chen, W., and Wei, G. (2016). Bacterial communities in oil contaminated soils: Biogeography and co-occurrence patterns. *Soil Biol. Biochem.* 98, 64–73. doi: 10.1016/j.soilbio.2016.04.005

Johnson, N. C., Angelard, C., Sanders, I. R., and Kiers, E. T. (2013). Predicting community and ecosystem outcomes of mycorrhizal responses to global change. *Ecol. Lett.* 16, 140–153. doi: 10.1111/ele.12085

Johnston, S. G., Bennett, W. W., Doriean, N., Hockmann, K., Karimian, N., and Burton, E. D. (2020). Antimony and arsenic speciation, redox-cycling and contrasting mobility in a mining-impacted river system. *Sci. Total Environ.* 710:136354. doi: 10.1016/j.scitotenv.2019.136354

Karanika, E. D., Voulgari, O. K., Mamolos, A. P., Alifragis, D. A., and Veresoglou, D. S. (2008). Arbuscular mycorrhizal fungi in northern Greece and influence of soil resources on their colonization. *Pedobiologia* 51, 409–418. doi: 10.1016/j.pedobi.2007.11.002

Kiers, E. T., Duhamel, M., Beesetty, Y., Mensah, J. A., Franken, O., Verbruggen, E., et al. (2011). Reciprocal rewards stabilize cooperation in the mycorrhizal symbiosis. *Science* 333, 880–882. doi: 10.1126/science.1208473

Kohout, P., Sudová, R., Janoušková, M., Čtvrtlíková, M., Hejda, M., Pánková, H., et al. (2014). Comparison of commonly used primer sets for evaluating arbuscular mycorrhizal fungal communities: Is there a universal solution? *Soil Biol. Biochem.* 68, 482–493. doi: 10.1016/j.soilbio.2013.08.027

Krishnamoorthy, R., Kim, C. G., Subramanian, P., Kim, K. Y., Selvakumar, G., and Sa, T. M. (2015). Arbuscular mycorrhizal fungi community structure, abundance and species richness changes in soil by different levels of heavy metal and metalloid concentration. *PLoS One* 10:e0128784. doi: 10.1371/journal.pone.0128784

Li, B., Xu, R., Sun, X., Han, F., Xiao, E., Chen, L., et al. (2021). Microbiome-environment interactions in antimony-contaminated rice paddies and the correlation of core microbiome with arsenic and antimony contamination. *Chemosphere* 263:128227. doi: 10.1016/j.chemosphere.2020.128227

Li, H., Gao, M. Y., Mo, C. H., Wong, M. H., Chen, X. W., and Wang, J. J. (2022). Potential use of arbuscular mycorrhizal fungi for simultaneous mitigation of arsenic and cadmium accumulation in rice. *J. Exp. Bot.* 73, 50–67. doi: 10.1093/jxb/erab444

Li, X., Yang, H., Zhang, C., Zeng, G., Liu, Y., Xu, W., et al. (2017). Spatial distribution and transport characteristics of heavy metals around an antimony mine area in central China. *Chemosphere* 170, 17–24. doi: 10.1016/j.chemosphere.2016.12.011

Li, Y., Lin, H., Gao, P., Yang, N., Xu, R., Sun, X., et al. (2021). Variation in the diazotrophic community in a vertical soil profile contaminated with antimony and arsenic. *Environ. Pollut.* 291:118248. doi: 10.1016/j.envpol.2021.118248

Liu, B., Wu, F., Li, X., Fu, Z., Deng, Q., Mo, C., et al. (2011). Arsenic, antimony and bismuth in human hair from potentially exposed individuals in the vicinity of antimony mines in Southwest China. *Microchem. J.* 97, 20–24. doi: 10.1016/j.microc.2010.07.008

Liu, Y. Q., Wen-Xin, L., Zhong-Qiu, Z., Yang, Y. P., Zhang, L. X., Wang, L. Y., et al. (2022). Aluminum adsorption and antimonite oxidation dominantly regulate antimony solubility in soils. *Chemosphere* 309:136651. doi: 10.1016/j.chemosphere.2022.136651

Liu, Y., Imtiaz, M., Ditta, A., Rizwan, M. S., Ashraf, M., Mehmood, S., et al. (2020). Response of growth, antioxidant enzymes and root exudates production towards As stress in *Pteris vittata* and in *Astragalus sinicus* colonized by arbuscular mycorrhizal fungi. *Environ. Sci. Pollut. Res. Int.* 27, 2340–2352. doi: 10.1007/s11356-019-06785-5

Long, L. K., Yao, Q., Guo, J., Yang, R. H., Huang, Y. H., and Zhu, H. H. (2010). Molecular community analysis of arbuscular mycorrhizal fungi associated with five selected plant species from heavy metal polluted soils. *Eur. J. Soil Biol.* 46, 288–294. doi: 10.1016/j.ejsobi.2010.06.003

Malcová, R., Vosátka, M., and Gryndler, M. (2003). Effects of inoculation with Glomus intraradices on lead uptake by *Zea mays L.* and *Agrostis capillaris L. Appl. Soil Ecol.* 23, 55–67. doi: 10.1016/s0929-1393(02)00160-9

Mao, K., Zhang, G., Wang, Q., Wu, Z., and Zhou, Y. (2022). Leaching characteristics of Sb and As from smelting slag in antimony mining area _ Influence of pH. *Earth Environ.* 51, 102–107. doi: 10.14050/j.cnki.1672-9250.2022.50.057

Ministry of Ecology and Environment of the People's Republic of China (2018). *Soil environmental quality: Risk control standard for soil contamination of development land.* Beijing: Ministry of Ecology and Environment of the People's Republic of China.

Moradi, M., Naji, H. R., Imani, F., Moradi Behbahani, S., and Ahmadi, M. T. (2017). Arbuscular mycorrhizal fungi changes by afforestation in sand dunes. *J. Arid Environ.* 140, 14–19. doi: 10.1016/j.jaridenv.2017.01.006

Nishad, P. A., and Bhaskarapillai, A. (2021). Antimony, a pollutant of emerging concern: A review on industrial sources and remediation technologies. *Chemosphere* 277:130252. doi: 10.1016/j.chemosphere.2021.130252

Okkenhaug, G., Zhu, Y. G., He, J., Li, X., Luo, L., and Mulder, J. (2012). Antimony (Sb) and arsenic (As) in Sb mining impacted paddy soil from Xikuangshan, China: Differences in mechanisms controlling soil sequestration and uptake in rice. *Environ. Sci. Technol.* 46, 3155–3162. doi: 10.1021/es2022472

Ozturk, M., Metin, M., Altay, V., Bhat, R. A., Ejaz, M., Gul, A., et al. (2022). Arsenic and human health: Genotoxicity, epigenomic effects, and cancer signaling. *Biol. Trace Elem. Res.* 200, 988–1001. doi: 10.1007/s12011-021-02719-w

Parniske, M. (2008). Arbuscular mycorrhiza: The mother of plant root endosymbioses. *Nat. Rev. Microbiol.* 6, 763–775. doi: 10.1038/nrmicro1987

Parvin, S., Van Geel, M., Yeasmin, T., Lievens, B., and Honnay, O. (2019). Variation in arbuscular mycorrhizal fungal communities associated with lowland rice (*Oryza sativa*) along a gradient of soil salinity and arsenic contamination in Bangladesh. *Sci. Total Environ.* 686, 546–554. doi: 10.1016/j.scitotenv.2019.05.450

Pawlowska, T. E., and Charvat, I. (2004). Heavy-metal stress and developmental patterns of arbuscular mycorrhizal fungi. *Appl. Environ. Microb.* 70, 6643–6649. doi: 10.1128/AEM.70.11.6643-6649.2004

Riaz, M., Kamran, M., Fang, Y., Wang, Q., Cao, H., Yang, G., et al. (2021). Arbuscular mycorrhizal fungi-induced mitigation of heavy metal phytotoxicity in metal contaminated soils: A critical review. *J. Hazard. Mater.* 402:123919. doi: 10.1016/j.jhazmat.2020.123919

Ruotsalainen, A. L., Markkola, A., and Kozlov, M. V. (2007). Root fungal colonisation in *Deschampsia flexuosa*: Effects of pollution and neighbouring trees. *Environ. Pollut.* 147, 723–728. doi: 10.1016/j.envpol.2006.09.004

Sanchez-Castro, I., Gianinazzi-Pearson, V., Cleyet-Marel, J. C., Baudoin, E., and van Tuinen, D. (2017). Glomeromycota communities survive extreme levels of metal toxicity in an orphan mining site. *Sci. Total Environ.* 598, 121–128. doi: 10.1016/j.scitotenv.2017.04.084

Schneider, J., Bundschuh, J., and do Nascimento, C. W. A. (2016). Arbuscular mycorrhizal fungi-assisted phytoremediation of a lead-contaminated site. *Sci. Total Environ.* 572, 86–97. doi: 10.1016/j.scitotenv.2016.07.185

Schneider, J., Sturmer, S. L., Guilherme, L. R., de Souza Moreira, F. M., and Soares, C. R. (2013). Arbuscular mycorrhizal fungi in arsenic-contaminated areas in Brazil. *J. Hazard. Mater.* 262, 1105–1115. doi: 10.1016/j.jhazmat.2012.09.063

Silva, D. F. D., Moreira, J. V., Sousa, L. I. S., Santana, M. C., Mota, J. C. A., Queiroz, A. D. S., et al. (2022). Arbuscular mycorrhizal fungi community in soils under desertification and restoration in the Brazilian semiarid. *Microbiol. Res.* 264:127161. doi: 10.1016/j.micres.2022.127161

Smith, S. E., Facelli, E., Pope, S., and Smith, F. A. (2009). Plant performance in stressful environments: Interpreting new and established knowledge of the roles of arbuscular mycorrhizas. *Plant Soil* 326, 3–20. doi: 10.1007/s11104-009-9981-5

Spruyt, A., Buck, M. T., Mia, A., and Straker, C. J. (2014). Arbuscular mycorrhiza (AM) status of rehabilitation plants of mine wastes in South Africa and determination of AM fungal diversity by analysis of the small subunit rRNA gene sequences. *S. Afr. J. Bot.* 94, 231–237. doi: 10.1016/j.sajb.2014.07.006

Stefanowicz, A. M., Kapusta, P., Zubek, S., Stanek, M., and Woch, M. W. (2020). Soil organic matter prevails over heavy metal pollution and vegetation as a factor shaping soil microbial communities at historical Zn-Pb mining sites. *Chemosphere* 240:124922. doi: 10.1016/j.chemosphere.2019.124922

Tang, J., Tang, X., Qin, Y., He, Q., Yi, Y., and Ji, Z. (2019). Karst rocky desertification progress: Soil calcium as a possible driving force. *Sci. Total Environ.* 649, 1250–1259. doi: 10.1016/j.scitotenv.2018.08.242

Teodoro, M., Hejcman, M., Vitkova, M., Wu, S., and Komarek, M. (2020). Seasonal fluctuations of Zn, Pb, As and Cd contents in the biomass of selected grass species growing on contaminated soils: Implications for in situ phytostabilization. *Sci. Total Environ.* 703:134710. doi: 10.1016/j.scitotenv.2019.134710

Van Geel, M., Jacquemyn, H., Plue, J., Saar, L., Kasari, L., Peeters, G., et al. (2018). Abiotic rather than biotic filtering shapes the arbuscular mycorrhizal fungal communities of European seminatural grasslands. *New Phytol.* 220, 1262–1272. doi: 10.1111/nph.14947

Vierheilig, H., Schweiger, P., and Brundrett, M. (2005). An overview of methods for the detection and observation of arbuscular mycorrhizal fungi in roots. *Physiol. Plant.* 125, 393–404. doi: 10.1111/j.1399-3054.2005.00564.x

Wei, Y., Chen, Z., Wu, F., Hou, H., Li, J., Shangguan, Y., et al. (2015a). Molecular diversity of arbuscular mycorrhizal fungi at a large-scale antimony mining area in southern China. *J. Environ. Sci.* 29, 18–26. doi: 10.1016/j.jes.2014.10.002

Wei, Y., Chen, Z., Wu, F., Li, J., ShangGuan, Y., Li, F., et al. (2015b). Diversity of arbuscular mycorrhizal fungi associated with a Sb accumulator plant, ramie (*Boehmeria nivea*), in an active Sb mining. *J. Microbiol. Biotechnol.* 25, 1205–1215. doi: 10.4014/jmb.1411.11033

Wei, Y., Su, Q., Sun, Z., Shen, Y., Li, J., Zhu, X., et al. (2016). The role of arbuscular mycorrhizal fungi in plant uptake, fractions, and speciation of antimony. *Appl. Soil Ecol.* 107, 244–250. doi: 10.1016/j.apsoil.2016.04.021

Wu, F., Fu, Z., Liu, B., Mo, C., Chen, B., Corns, W., et al. (2011). Health risk associated with dietary co-exposure to high levels of antimony and arsenic in the world's largest antimony mine area. *Sci. Total Environ.* 409, 3344–3351. doi: 10.1016/j.scitotenv.2011.05.033

Wu, J., Liang, J., Bjorn, L. O., Li, J., Shu, W., and Wang, Y. (2022). Phosphorus-arsenic interaction in the "soil-plant-microbe" system and its influence on arsenic pollution. *Sci. Total Environ.* 802:149796. doi: 10.1016/j.scitotenv.2021.149796

Wu, S., You, F., Wu, Z., Bond, P., Hall, M., and Huang, L. (2020). Molecular diversity of arbuscular mycorrhizal fungal communities across the gradient of alkaline Fe ore tailings, revegetated waste rock to natural soil sites. *Environ. Sci. Pollut. Res. Int.* 27, 11968–11979. doi: 10.1007/s11356-020-07780-x

Xi, L., Shen, Y., Zhao, X., Zhou, M., Mi, Y., Li, X., et al. (2022). Effects of arbuscular mycorrhizal fungi on frond antimony enrichment, morphology, and proteomics in *Pteris cretica* var. *nervosa* during antimony phytoremediation. *Sci. Total Environ.* 804:149904. doi: 10.1016/j.scitotenv.2021.149904

Xiao, B., Hu, K., Veste, M., and Kidron, G. J. (2019). Natural recovery rates of moss biocrusts after severe disturbance in a semiarid climate of the Chinese Loess Plateau. *Geoderma* 337, 402–412. doi: 10.1016/j.geoderma.2018.09.054

Xiao, D., He, X., Zhang, W., Cheng, M., Hu, P., and Wang, K. (2022). Diazotroph and arbuscular mycorrhizal fungal diversity and community composition responses to karst and non-karst soils. *Appl. Soil Ecol.* 170:104227. doi: 10.1016/j.apsoil.2021.104227

Xiao, D., Tan, Y., Liu, X., Yang, R., Zhang, W., He, X., et al. (2019). Effects of different legume species and densities on arbuscular mycorrhizal fungal communities in a karst grassland ecosystem. *Sci. Total Environ.* 678, 551–558. doi: 10.1016/j.scitotenv.2019.04.293

Xu, R., Sun, X., Han, F., Li, B., Xiao, E., Xiao, T., et al. (2020). Impacts of antimony and arsenic co-contamination on the river sedimentary microbial community in an antimony-contaminated river. *Sci. Total Environ.* 713:136451. doi: 10.1016/j.scitotenv.2019.136451

Yan, K., Abbas, M., Meng, L., Cai, H., Peng, Z., Li, Q., et al. (2021). Analysis of the fungal diversity and community structure in Sichuan dark tea during pile-fermentation. *Front. Microbiol.* 12:706714. doi: 10.3389/fmicb.2021.706714

Yan, K., Pei, Z., Meng, L., Zheng, Y., Wang, L., Feng, R., et al. (2022). Determination of community structure and diversity of seed-vectored endophytic fungi in *Alpinia zerumbet. Front. Microbiol.* 13:814864. doi: 10.3389/fmicb.2022.814864

Yan, T., Xue, J., Zhou, Z., and Wu, Y. (2021). Impacts of biochar-based fertilization on soil arbuscular mycorrhizal fungal community structure in a karst mountainous area. *Environ. Sci. Pollut. Res. Int.* 28, 66420–66434. doi: 10.1007/s11356-021-15499-6

Yang, R., Sun, W., Guo, L., Li, B., Wang, Q., Huang, D., et al. (2022). Response of soil protists to antimony and arsenic contamination. *Environ. Pollut.* 315:120387. doi: 10.1016/j.envpol.2022.120387

Yang, Y., Liang, Y., Han, X., Chiu, T. Y., Ghosh, A., Chen, H., et al. (2016). The roles of arbuscular mycorrhizal fungi (AMF) in phytoremediation and tree-herb interactions in Pb contaminated soil. *Sci. Rep.* 6:20469. doi: 10.1038/srep20469

Yang, Y., Song, Y., Scheller, H. V., Ghosh, A., Ban, Y., Chen, H., et al. (2015). Community structure of arbuscular mycorrhizal fungi associated with *Robinia pseudoacacia* in uncontaminated and heavy metal contaminated soils. *Soil Biol. Biochem.* 86, 146–158. doi: 10.1016/j.soilbio.2015.03.018

Yu, H., Zheng, X., Weng, W., Yan, X., Chen, P., Liu, X., et al. (2021). Synergistic effects of antimony and arsenic contaminations on bacterial, archaeal and fungal communities in the rhizosphere of *Miscanthus sinensis*: Insights for nitrification and carbon mineralization. *J. Hazard. Mater.* 411:125094. doi: 10.1016/j.jhazmat.2021.125094

Zarei, M., Hempel, S., Wubet, T., Schafer, T., Savaghebi, G., Jouzani, G. S., et al. (2010). Molecular diversity of arbuscular mycorrhizal fungi in relation to soil chemical properties and heavy metal contamination. *Environ. Pollut.* 158, 2757–2765. doi: 10.1016/j.envpol.2010.04.017

Zarei, M., Saleh-Rastin, N., Jouzani, G. S., Savaghebi, G., and Buscot, F. (2008). Arbuscular mycorrhizal abundance in contaminated soils around a zinc and lead deposit. *Eur. J. Soil Biol.* 44, 381–391. doi: 10.1016/j.ejsobi.2008.06.004

Zhan, F., Li, B., Jiang, M., Li, T., He, Y., Li, Y., et al. (2019). Effects of arbuscular mycorrhizal fungi on the growth and heavy metal accumulation of bermudagrass [*Cynodon dactylon (L.)* Pers.] grown in a lead-zinc mine wasteland. *Int. J. Phytoremediat.* 21, 849–856. doi: 10.1080/15226514.2019.1577353

Zhang, C., and Chen, Z. (2021). Advances in study on the effects of arbuscular mycorrhizal fungi on plants in remediation of arsenic-contaminated soil. *Acta Agr. Scand. B Soil Plant Sci.* 71, 825–834. doi: 10.1080/09064710.2021.1952300

Zhang, S., Luo, P., Yang, J., Irfan, M., Dai, J., An, N., et al. (2021). Responses of arbuscular mycorrhizal fungi diversity and community to 41-year rotation fertilization in brown soil region of Northeast China. *Front. Microbiol.* 12:742651. doi: 10.3389/fmicb.2021.742651

Zhang, Z., Wang, H., Song, X., Liang, Z., and Tang, Z. (2019). Arbuscular mycorrhizal fungal diversity is affected by soil salinity and soil nutrients in typical saline-sodic grasslands dominated by *Leymus chinensis. Arid Land Res. Manag.* 34, 68–82. doi: 10.1080/15324982.2019.1631405

Zhou, M., Li, X., Liu, X., Mi, Y., Fu, Z., Zhang, R., et al. (2022). Effects of antimony on rice growth and its existing forms in rice under arbuscular mycorrhizal fungi environment. *Front. Microbiol.* 13:814323. doi: 10.3389/fmicb.2022.814323